

Hot Jupiters are asynchronous rotators

MAREK WAZNY^{1,2} AND KRISTEN MENO^{1,2,3,4}

¹*David A. Dunlap Department of Astronomy & Astrophysics, University of Toronto, 50 St. George Street, Toronto, Ontario, M5S 3H4, Canada*

²*Department of Physics, University of Toronto, 60 St George Street, Toronto, Ontario, M5S 1A7, Canada*

³*Physics & Astrophysics Group, Dept. of Physical & Environmental Sciences, University of Toronto Scarborough, 1265 Military Trail, Toronto, Ontario, M1C 1A4, Canada*

⁴*Observatoire de la Cote d'Azur, TOP team, Laboratoire Lagrange - CNRS, Nice, France*

ABSTRACT

Hot Jupiters are typically assumed to be synchronously rotating, from tidal locking. Their thermally-driven atmospheric winds experience Lorentz drag on the planetary magnetic field anchored at depth. We find that the magnetic torque does not integrate to zero over the entire atmosphere. The resulting angular momentum feedback on the bulk interior can thus drive the planet away from synchronous rotation. Using a toy tidal-ohmic model and atmospheric GCM outputs for HD189733b, HD209458b and Kepler7b, we establish that off-synchronous rotation can be substantial at tidal-ohmic equilibrium for sufficiently hot and/or magnetized hot Jupiters. Potential consequences of asynchronous rotation for hot Jupiter phenomenology motivate follow-up work on the tidal-ohmic scenario with approaches that go beyond our toy model.

1. INTRODUCTION

Hot Jupiters, a class of exoplanets with masses and radii comparable to Jupiter but with orbital periods less than 10 days, present a long-standing problem known as the 'radius anomaly'. A significant fraction of these planets possess radii in excess of ~ 1.2 Jupiter radii (Charbonneau et al. 1999; Henry et al. 1999), a phenomenon that cannot be interpreted by the standard theory of planetary evolution. This discrepancy between observed and theoretical radii is often referred to as the radius inflation problem. Several interpretations have been proposed to explain this anomaly, including tidal heating (Bodenheimer et al. 2001; Bodenheimer et al. 2003; Ibgui & Burrows 2009; Ibgui et al. 2010), Ohmic heating (Batygin & Stevenson 2010; Showman et al. 2010; Perna et al. 2010a,b), inward transfer of irradiation (Tremblin et al. 2017; Sainsbury-Martinez et al. 2019), and high opacity (Burrows et al. 2007). Despite these proposals, the radius inflation problem for hot Jupiters remains one of the outstanding unresolved issues in our understanding of extrasolar planets (Sarkis, P. et al. 2021).

Ohmic heating has emerged as a promising solution to the radius inflation problem. This mechanism, which involves the dissipation of electrical currents in the conductive interiors of these planets, has been successful in explaining the inflated radii of many hot Jupiters. However, it falls short when applied to the most inflated planets, indicating that additional processes may be at play (Huang & Cumming 2012). The focus of the the-

ory has largely been energetic aspects like Joule heating at depth to inflate the planets. However, there is also a need to consider the effects of drag and momentum balance in this context. In particular, the zonal winds in the atmosphere, which are driven by thermal gradients, experience drag as they interact with the planetary magnetic field. This means that any net momentum that is removed from the atmosphere must be deposited somewhere else, possibly deeper in the planet.

In this work, we make the straightforward assumption that the net momentum that is removed from the atmosphere is deposited in the bulk interior. This implies that the bulk of the planet can be torqued as a result of the magnetic drag acting in the atmosphere. This leads to the possibility of asynchronous rotation for the bulk planetary interior, a scenario that has not been extensively explored in the context of hot Jupiters.

We investigate this tidal-ohmic scenario with a toy model, combining tidal theory with simple momentum balance arguments. Our model relaxes the assumption of synchronous rotation and indeed suggests the possibility of significant asynchronous rotation, for sufficiently hot and magnetized hot Jupiters. The tidal-ohmic scenario opens up new avenues for understanding hot Jupiter observables by providing a channel for strong coupling between the interior and the atmosphere of these planets.

2. SIMULATED ATMOSPHERES

We employ PlaSim-Gen as a general circulation model (GCM) for tidally locked gas giants that simulates their

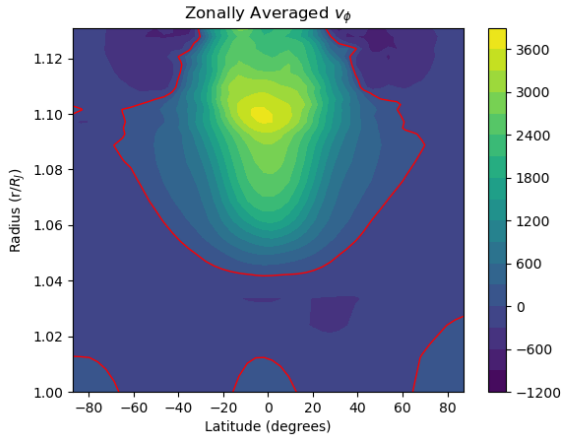


Figure 1. Zonally-averaged zonal wind speeds of planet Kepler7b generated by the GCM. Wind speeds are shown in m s^{-1} where the red line separates regions of opposite wind directions.

atmospheric dynamics and was adapted for hot Jupiters by considering sufficiently hot atmospheres. This model solves meteorological fluid equations on atmospheric pressure levels to evolve temperature, density, and wind velocity fields. These fields are solved for 1200 planet days until a near equilibrium is found, then we extract an average of the data over the last four days. For further model details see [Paradise et al. \(2022\)](#); [Menou \(2020\)](#), and see [Menou \(2022\)](#) for the specific data used throughout this work.

Simulated temperature and velocity fields from observed planets HD189733b, HD209458b, and Kepler7b are used to extrapolate other relevant properties for this analysis. Note that each field is evaluated as a function of pressure (1 mbar to 100 bar), latitude, and longitude. Where relevant, pressure is converted to radial coordinates via the ideal gas law

$$\frac{dp}{dr} = -g \frac{\mu m_H}{kT} p, \quad (1)$$

assuming constant gravitational acceleration, g and mean molecular weight μ . Hot Jupiter atmosphere composition is approximately solar ([Hansen & Barman 2007](#)). We thus adopt $\mu = 2.4$ throughout our analysis. Figure 1 shows the zonal wind in radius coordinates for planet Kepler7b.

The base radius for the deepest point of the atmosphere is approximated as 1 Jupiter radius. We confirmed that modifying this base radius by 10% has minimal effect on the general conclusions of this paper. We assume a radiative-convective boundary located at 100 bar for simplicity, although this would need to be computed together with thermal state ([Fortney et al. 2021](#)).

3. MAGNETIC EFFECTS

3.1. Density, Ionization, and Resistivity

To determine the density of the atmosphere we assume an ideal gas law. The atmospheric gas densities have mean values $1.12 \times 10^{-4} \text{ g cm}^{-3}$ for HD189733b and HD209458b while $1.22 \times 10^{-4} \text{ g cm}^{-3}$ for Kepler7b. The variation in density is about 5 orders of magnitude with minimum values around $\sim 10^{-8} \text{ g cm}^{-3}$ in the upper atmosphere and maximum values reaching $\sim 10^{-3} \text{ g cm}^{-3}$ in the deeper atmosphere. This is typical of most hot Jupiters atmospheres. See also in [Perna et al. \(2010a\)](#).

Hot Jupiter temperatures roughly range from 1000 \sim 3000 K, hence thermal ionization of alkali metals provide the free electric charges. To estimate the ionization fraction, x_e , in a weakly ionized regime, the Saha equation is recast into a single ionization form ([Sato 1991](#)),

$$x_e \equiv \frac{n_e}{n_n} = \sum_j \frac{n_j}{n} x_j, \quad (2)$$

$$\frac{x_j^2}{1 - x_j^2} \simeq \frac{1}{n_j kT} \left(\frac{2\pi m_e}{h^2} \right)^{3/2} (kT)^{5/2} \exp\left(-\frac{I_j}{kT}\right),$$

where n_e and n_n are the number densities of electrons and neutrals, n_j is the number density of element j , I_j is the corresponding first ionization potential, T is the temperature, n is the total number density of the gas, and k, m_e, h are the usual constants. We use the first 28 elements of the periodic table (H to Ni) for the ionization potentials, assuming solar abundances. This solution for the ionization fraction allows the electric resistivity to be evaluated everywhere in the atmosphere as

$$\eta = 230 \frac{\sqrt{T}}{x_e} \text{ cm}^2 \text{ s}^{-1}. \quad (3)$$

Given the GCM temperature and density fields, the mean resistivity values are $2.76 \times 10^{29} \text{ cm}^2 \text{ s}^{-1}$, $2.26 \times 10^{29} \text{ cm}^2 \text{ s}^{-1}$ for HD189733b, HD209458b and $1.48 \times 10^{27} \text{ cm}^2 \text{ s}^{-1}$ for Kepler7b, with orders-of-magnitude spatial variations. Minimum values are similar for all planets $\sim 10^{12} \text{ cm}^2 \text{ s}^{-1}$, while maximum values are $\sim 10^{33} \text{ cm}^2 \text{ s}^{-1}$ for HD189733b and $\sim 10^{31} \text{ cm}^2 \text{ s}^{-1}$ for Kepler7b and HD209458b.

3.2. Induced Current and Magnetic Drag Time

It is believed that magnetic fields in hot Jupiters arise in a similar manner to that of Jupiter and Saturn, through an interior convection-driven dynamo. We assume the magnetic field geometry to be purely poloidal, in the form of an aligned dipole;

$$\mathbf{B}_{\text{dip}}(\mathbf{r}) = B_0(2 \cos \theta \mathbf{e}_r + \sin \theta \mathbf{e}_\theta), \quad (4)$$

where B_0 is the field strength.

Charged zonal winds deform the poloidal magnetic field, generating a toroidal (east-west) component. The toroidal field obeys the resistive induction equation,

$$\begin{aligned} \frac{\partial B_\phi}{\partial t} = & r \sin \theta \left[\frac{\partial \Omega}{\partial r} B_r + \frac{1}{r} \frac{\partial \Omega}{\partial \theta} B_\theta \right] + \frac{1}{r} \frac{\partial}{\partial r} \left[\eta \frac{\partial}{\partial r} (r B_\phi) \right] \\ & + \frac{1}{r^2} \frac{\partial}{\partial \theta} \left[\frac{\eta}{\sin \theta} \frac{\partial}{\partial \theta} (\sin \theta B_\phi) \right], \end{aligned} \quad (5)$$

where $\Omega = v_\phi(r \sin \theta)^{-1}$ and v_ϕ is the zonal wind speed. Because the entire velocity field, \mathbf{v} , is dominated by v_ϕ from largely zonal jets, we narrow our analysis by neglecting gradient poloidal terms $\partial/\partial\theta$ in Equation (5). This is consistent with neglecting the magnetic drag applied to the meridional (north-south) winds, which are small.

An alternative view of the MHD problem is that an induced current \mathbf{j} , is supporting the induced toroidal field. The benefits of this approach will become clear below. Neglecting poloidal terms in the induction equation is equivalent to $\mathbf{j}_\theta \gg \mathbf{j}_r$. Imposing steady state to Equation (5) leads to the induced current (Liu et al. 2008),

$$\begin{aligned} j_\theta(r, \theta, \phi) = & -\frac{c \sin \theta}{4\pi r \eta} \int_r^R dr' r'^2 \left(\frac{\partial \Omega}{\partial r'} B_r + \frac{1}{r'} \frac{\partial \Omega}{\partial \theta} B_\theta \right) \\ & + \frac{R}{r \eta} [\eta j_\theta]_{r=R}, \end{aligned} \quad (6)$$

where the resistivity, $\eta(r, \theta, \phi)$ depends on position through temperature, and $[\eta j_\theta]_{r=R}$ is an outer boundary condition related to the ionosphere.

We will ignore this last term. Although this is a valid assumption in neutral-top atmospheres (such as those of Jupiter and Saturn) with a top insulating boundary, in the ionized atmospheres of hot Jupiters this assumption may not hold. We address this by simply noting that any additional contribution from this term may increase the magnetic drag and hence the total torque. As our work is concerned with setting up a minimum threshold for asynchronous rotation, neglecting this term is a reasonable working assumption.

Previous works (Perna et al. 2010a; Menou 2012), evaluate this induced current through an order of magnitude approximation: $j_\theta \sim c v_\phi B_0 / (4\pi \eta)$. Here, we numerically integrate Equation (6) using the data in section 2, without the boundary term. Figure 2 compares these two approaches to determining j_θ averaged across longitude.

The positive contributions are very similar in geometry for the approximate and integral forms of the induced current. Also, both treatments produce a

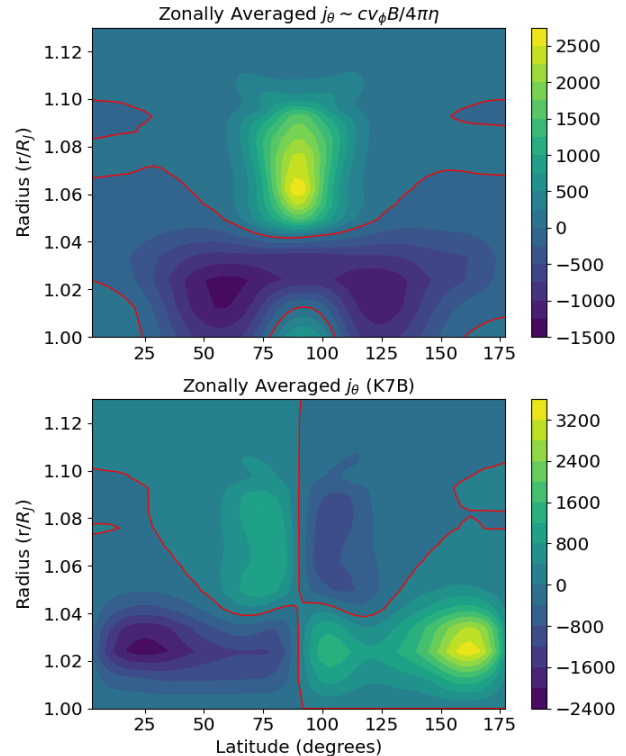


Figure 2. Numerically evaluated induced current (cgs units, scaled) for averaged zonally with red lines separating positive and negative regions. Top: Approximated current. Bottom: Numerically integrated current (Equation 6) with zero boundary term. Both plots are for the planet Kepler7b, assuming a magnetic field strength of 10 G.

counter-current, with a similar mean value in both treatments.

With the induced current, we can analyze the magnetic field effects on zonal winds. In general, calculating this effect requires solving MHD equations, for example as in Rogers & Showman (2014). However, our approach estimates MHD effects through the timescale, τ_{drag} . This timescale evaluates the effective time for the zonal winds to reach stationarity against the toroidal magnetic field.

A magnitude estimate for the drag timescale can be found by adopting an ion drag formulation, as outlined in Zhu et al. (2005). Using the estimate that the momentum carried by the wind is proportional to the Lorentz force, while assuming $j_\theta \sim c v_\phi B_0 / (4\pi \eta)$, leads to the order of magnitude approximation,

$$\tau_{\text{drag}} \sim \frac{4\pi \rho \eta}{B_0^2 \cos \theta}. \quad (7)$$

Using Equation (7), magnetic drag has been found to be significant in the atmospheres of hot Jupiters (Perna et al. 2010a). This work expands on the approximation

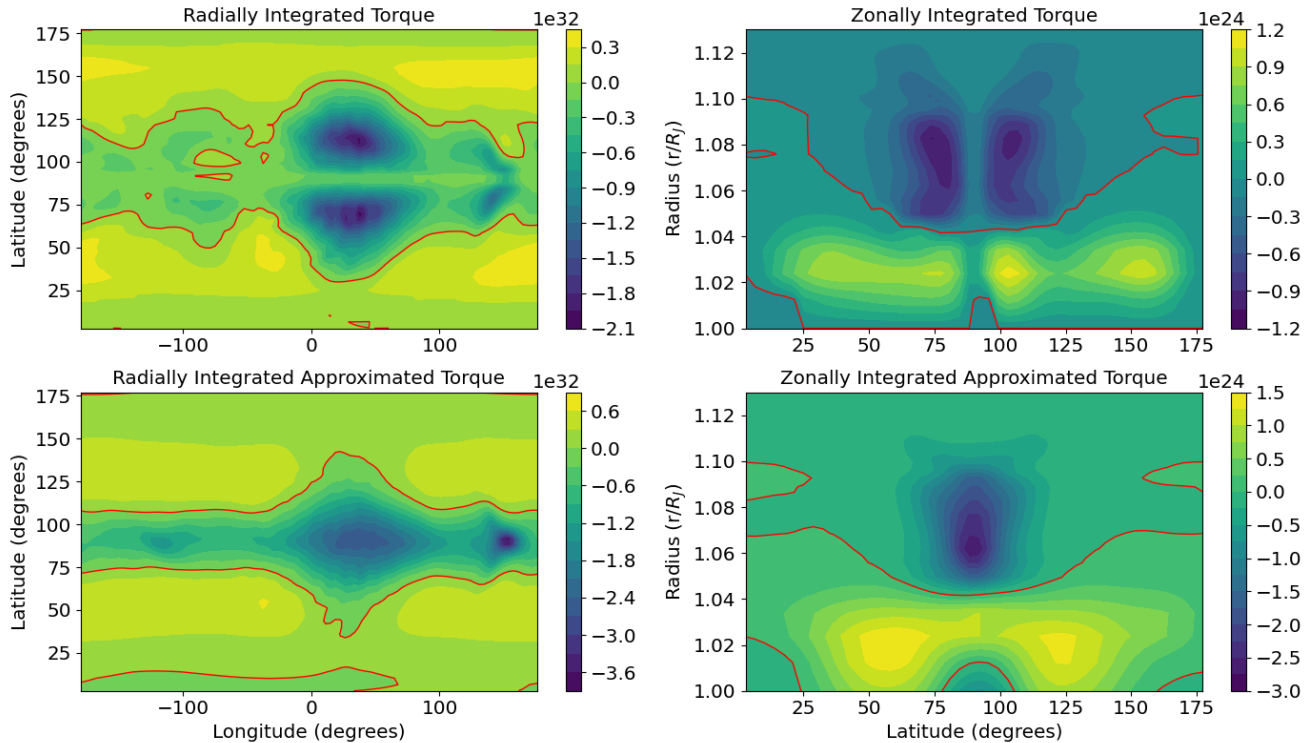


Figure 3. Left: Magnetic torque (dyne cm) of planet Kepler7b radially evaluating Equation 9 for the approximate drag time in Equation 7 (bottom) and Equation 8 (top). Right: Magnetic torque of planet Kepler7b zonally integrated for the approximate (bottom) and integrated (top) drag times. Red lines separate regions of positive and negative contributions.

by using the induced current obtained in section 3.2 to calculate the drag time more consistently through

$$\tau_{\text{drag}} \sim \frac{\rho |v_{\phi}| c}{|\mathbf{j}_{\theta} \times \mathbf{B}|}. \quad (8)$$

Using this new prescription for the drag time, results still generally agree with those reported in Perna et al. (2010a), with a few notable differences. This includes longer drag times deeper in the atmosphere and on the night-side, as well as shorter drag times on the day side. A notable difference occurs at the equator, where drag times are longer in the new treatment of the induced current.

3.3. Magnetic Torque

The magnetic drag timescale approximates the drag experienced by the winds as a linear term which takes the form $v_{\phi}/\tau_{\text{drag}}$.

Drag forces induce a torque on the atmosphere which determines the momentum transfer from the MHD effects on the wind. Using the linear drag term, the total magnetic torque can be computed as

$$\Gamma_{\text{tot}} = - \int d^3\mathbf{r} \rho(\mathbf{r}) \mathbf{r} \frac{v_{\phi}(\mathbf{r})}{\tau_{\text{drag}}(\mathbf{r})}. \quad (9)$$

In Equation (9) integration is done over the atmosphere, rather than the entire planet since no wind is present in

the bulk interior, by design. Our sign convention highlights that the total torque works against the dominant winds.

Figure 3 visualizes the magnitude of the torque field, comparing treatments of the drag timescales in Equations (7) and (8). The greatest contributions occur where zonal jets and higher temperatures are present. The right side of Figure 3 shows that the geometry of the induced current in Figure 2 largely determines the geometry of the zonal torque.

4. TIDAL-OHMIC SCENARIO

We posit that the total torque experienced by the atmospheric winds exerts a continuous reciprocal torque on the bulk rotation rate of the planet. This assumes no external loss of angular momentum such as in an outflowing MHD wind. Conservation of angular momentum across the atmosphere and interior regions implies deposition of angular momentum (via a positive torque contribution) in the core of the planet, where it would presumably be well mixed by convective motions. While we do not detail a specific mechanism for this momentum transfer, perturbed magnetic field lines rooted in the planet's interior dynamo region are prime candidates (see, e.g., Appendix in Wu & Lithwick 2012).

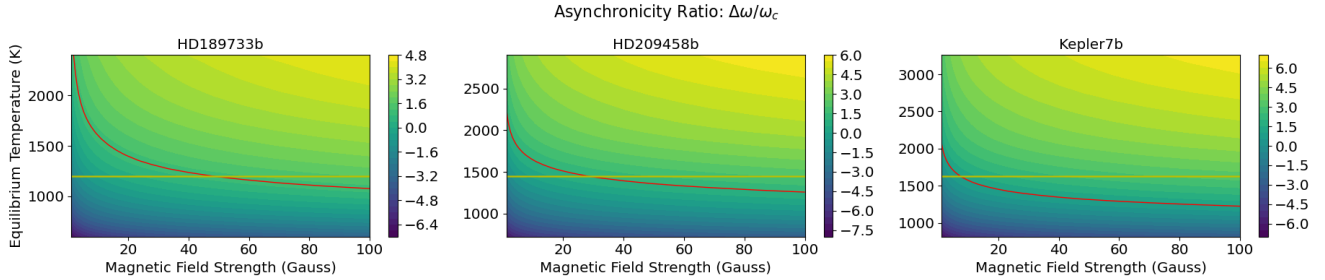


Figure 4. Asynchronicity ratio, $\Delta\omega/\omega_c$, for planets HD189733b, HD209458b, and Kepler7b. Values are calculated given an equilibrium temperature and magnetic field strength. Red lines correspond to the isolines $\Delta\omega/\omega_c = 1$ while yellow lines show the equilibrium temperature for each planet.

Conservation of angular momentum in the atmosphere yields $d(I_a\omega_a)/dt = -\Gamma_{\text{tot}}$, where I_a is the moment of inertia and ω_a is the angular frequency of the atmosphere. For simplicity, we assume that the planet does not deform, hence I_a is constant.

For the core dynamics, with core mass M_c and radius R_c , we adopt the time-independent moment of inertia of a solid sphere, $I_c \sim 2M_cR_c^2/5$. The synchronous angular frequency, ω_{sync} , is equal to the orbital frequency, so that the degree of asynchronicity (off-synchronous frequency) can be written as $\Delta\omega = \omega_c - \omega_{\text{sync}}$. We neglect any tides in the atmosphere and assume that tides only act on the angular frequency of the core, ω_c . By analogy with magnetic drag, we introduce a tidal timescale, τ_{tide} , which represents the typical timescale on which the core's angular frequency is synchronized by tidal effects. Following Hansen (2010) and Hansen (2012), for an orbital period P , and a tidal dissipation parameter Q , the tidal timescale can be written as $\tau_{\text{tide}} \sim QP$ where

$$Q = 3.0 \times 10^8 \left(\frac{a}{0.1 \text{ AU}} \right)^{3/2} \left(\frac{R_p}{1 R_J} \right)^{-5} \left(\frac{M_*}{M_\odot} \right)^{-1/2}. \quad (10)$$

Here a is the semi-major axis, R_p is the radius of the planet, and M_* is the mass of the host star.

Given this tidal timescale, conservation of angular momentum for the core yields

$$I_c \frac{d\omega_c}{dt} = \Gamma_{\text{tot}} + \frac{2}{5} M_c R_c^2 \frac{\Delta\omega}{\tau_{\text{tide}}}, \quad (11)$$

under the combined action of tidal and magnetic torques. At steady state, $d\omega_c/dt = 0$, so that the off-synchronous frequency can be evaluated from the total torque entering Equation (11) as

$$\Delta\omega = -\frac{5}{2} \frac{\tau_{\text{tide}}}{M_c R_c^2} \Gamma_{\text{tot}}. \quad (12)$$

When the off-synchronous angular frequency, $\Delta\omega$, approaches or exceeds the magnitude of the orbital frequency, ω_{sync} , tidal locking is significantly disrupted.

We address this possibility for the planets Kepler-7b, HD189733b, and HD209458b, with estimates of $\Delta\omega$ for each planet reported in Table 1, under the assumption of 10 G magnetic field strength.

For simplicity, we assume $M_* = M_\odot$ with parameters $a = 0.0313$ au, $P = 1.9 \times 10^5$ s for HD189733b, $a = 0.0463$ au, $P = 3.04 \times 10^5$ s for HD209458b (Rosenthal et al. 2021), and $a = 0.0624$ au, $P = 4.2 \times 10^5$ s for Kepler7b (Latham et al. 2010). Consider the case of Kepler7b with an orbital frequency of $1.5 \times 10^{-5} \text{ s}^{-1}$. This is much smaller than the off-synchronous frequency reported in Table 1, indicating potentially strong asynchronicity for this specific hot Jupiter. By contrast, HD189733b has an orbital frequency of $3.3 \times 10^{-5} \text{ s}^{-1}$, larger than the off-synchronous frequency reported in Table 1. This amounts to a small, but non-negligible amount of asynchronicity, even for this cooler planet.

Equilibrium temperatures near or above 1500 K appear to be needed for strong tidal-ohmic effects, unless the planetary magnetic field strengths are well in excess of the 10 G assumed here. Figure 4 provides an asynchronicity ratio, $\Delta\omega/\omega_c$, demonstrating the equilibrium temperatures and magnetic field strengths needed for strong asynchronous rotation.

5. CONCLUSION

Our work challenges the assumption of synchronous rotation for hot Jupiters in the presence of atmospheric Lorentz drag. The net angular momentum torque mediated by the planetary field lines does not cancel out over the atmosphere, suggesting that the reciprocal torque could drive the bulk interior away from synchronous rotation. We find that this off-synchronous rotation can be significant, particularly in hot Jupiters that are sufficiently hot and/or have strong magnetic fields. These findings are supported by a tidal-ohmic toy model, in combination with atmospheric GCM outputs for planets HD189733b, HD209458b, and Kepler7b, showing that the degree of asynchronicity is notable at tidal-ohmic equilibrium.

Table 1. Below are the mean planet characteristics and magnetic properties for planets HD189733b, HD209458b, and Kepler7b. The magnetic field is assumed to have a dipole geometry with a strength of 10 Gauss for each planet.

Parameter	HD189733b	HD209458b	Kepler7b	Description
g	2200	800	414	Gravitational acceleration (cm s^{-1})
T_{eq}	1200	1450	1630	Equilibrium temperature (K)
$\bar{\rho}$	1.18×10^{-3}	1.17×10^{-3}	1.22×10^{-3}	Mean density (g cm^{-3})
$\bar{\eta}$	2.76×10^{29}	2.26×10^{27}	1.48×10^{27}	Mean resistivity ($\text{cm}^2 \text{s}^{-1}$)
$\bar{\tau}_{\text{drag}}$	3.24×10^{22}	5.02×10^{19}	1.41×10^{19}	Mean drag time (s)
Γ_{tot}	-5.89×10^{31}	-5.19×10^{31}	-3.59×10^{32}	Total torque (dyne cm)
$\Delta\omega$	1.4×10^{-5}	3.6×10^{-5}	3.2×10^{-4}	Off-synchronous frequency (rad s^{-1})

This work highlights the need to re-evaluate the rotational states of hot Jupiters and consider the broad implications of asynchronous rotation on observable properties, such as atmospheric features and phase curves (Rauscher & Kempton 2014). Our results motivate further research with more comprehensive models of the tidal-ohmic scenario, which could yield deeper insights into the physical processes governing hot Jupiters, including the longstanding radius inflation problem.

ACKNOWLEDGEMENTS

KM is supported by the National Science and Engineering Research Council of Canada. KM thanks C. Gammie for sharing an early implementation of the Saha ionization balance solver used in this work.

We would furthermore like to acknowledge that this work was performed on land which for thousands of years has been the traditional land of the Huron-Wendat, the Seneca and the Mississaugas of the Credit. Today this meeting place is still the home to many indigenous people from across Turtle Island and we are grateful to have the opportunity to work on this land.

REFERENCES

- Batygin, K., & Stevenson, D. J. 2010, *The Astrophysical Journal Letters*, 714, L238, doi: [10.1088/2041-8205/714/2/L238](https://doi.org/10.1088/2041-8205/714/2/L238)
- Bodenheimer, P., Laughlin, G., & Lin, D. N. C. 2003, *The Astrophysical Journal*, 592, 555, doi: [10.1086/375565](https://doi.org/10.1086/375565)
- Bodenheimer, P., Lin, D. N. C., & Mardling, R. A. 2001, *ApJ*, 548, 466, doi: [10.1086/318667](https://doi.org/10.1086/318667)
- Burrows, A., Hubeny, I., Budaj, J., & Hubbard, W. B. 2007, *ApJ*, 661, 502, doi: [10.1086/514326](https://doi.org/10.1086/514326)
- Charbonneau, D., Brown, T. M., Latham, D. W., & Mayor, M. 1999, *The Astrophysical Journal*, 529, L45, doi: [10.1086/312457](https://doi.org/10.1086/312457)
- Fortney, J. J., Dawson, R. I., & Komacek, T. D. 2021, *Journal of Geophysical Research: Planets*, 126, e2020JE006629, doi: <https://doi.org/10.1029/2020JE006629>
- Hansen, B. M. S. 2010, *ApJ*, 723, 285, doi: [10.1088/0004-637X/723/1/285](https://doi.org/10.1088/0004-637X/723/1/285)
- Hansen, B. M. S. 2012, *The Astrophysical Journal*, 757, 6, doi: [10.1088/0004-637X/757/1/6](https://doi.org/10.1088/0004-637X/757/1/6)
- Hansen, B. M. S., & Barman, T. 2007, *The Astrophysical Journal*, 671, 861, doi: [10.1086/523038](https://doi.org/10.1086/523038)
- Henry, G. W., Marcy, G. W., Butler, R. P., & Vogt, S. S. 1999, *The Astrophysical Journal*, 529, L41, doi: [10.1086/312458](https://doi.org/10.1086/312458)
- Huang, X., & Cumming, A. 2012, *The Astrophysical Journal*, 757, 47, doi: [10.1088/0004-637X/757/1/47](https://doi.org/10.1088/0004-637X/757/1/47)
- Ibgui, L., & Burrows, A. 2009, *The Astrophysical Journal*, 700, 1921, doi: [10.1088/0004-637X/700/2/1921](https://doi.org/10.1088/0004-637X/700/2/1921)
- Ibgui, L., Burrows, A., & Spiegel, D. S. 2010, *The Astrophysical Journal*, 713, 751, doi: [10.1088/0004-637X/713/2/751](https://doi.org/10.1088/0004-637X/713/2/751)
- Latham, D. W., Borucki, W. J., Koch, D. G., et al. 2010, *The Astrophysical Journal Letters*, 713, L140, doi: [10.1088/2041-8205/713/2/L140](https://doi.org/10.1088/2041-8205/713/2/L140)
- Liu, J., Goldreich, P. M., & Stevenson, D. J. 2008, *Icarus*, 196, 653, doi: <https://doi.org/10.1016/j.icarus.2007.11.036>
- Menou, K. 2012, *The Astrophysical Journal*, 745, 138, doi: [10.1088/0004-637X/745/2/138](https://doi.org/10.1088/0004-637X/745/2/138)
- . 2020, *Monthly Notices of the Royal Astronomical Society*, 493, 5038, doi: [10.1093/mnras/staa532](https://doi.org/10.1093/mnras/staa532)
- . 2022, *Monthly Notices of the Royal Astronomical Society*, 517, 2714, doi: [10.1093/mnras/stac2854](https://doi.org/10.1093/mnras/stac2854)
- Paradise, A., Macdonald, E., Menou, K., Lee, C., & Fan, B. L. 2022, *Monthly Notices of the Royal Astronomical Society*, 511, 3272, doi: [10.1093/mnras/stac172](https://doi.org/10.1093/mnras/stac172)
- Perna, R., Menou, K., & Rauscher, E. 2010a, *The Astrophysical Journal*, 719, 1421, doi: [10.1088/0004-637x/719/2/1421](https://doi.org/10.1088/0004-637x/719/2/1421)

- . 2010b, *The Astrophysical Journal*, 724, 313,
doi: [10.1088/0004-637X/724/1/313](https://doi.org/10.1088/0004-637X/724/1/313)
- Rauscher, E., & Kempton, E. M. R. 2014, *ApJ*, 790, 79,
doi: [10.1088/0004-637X/790/1/79](https://doi.org/10.1088/0004-637X/790/1/79)
- Rogers, T. M., & Showman, A. P. 2014, *The Astrophysical Journal Letters*, 782, L4,
doi: [10.1088/2041-8205/782/1/L4](https://doi.org/10.1088/2041-8205/782/1/L4)
- Rosenthal, L. J., Fulton, B. J., Hirsch, L. A., et al. 2021,
ApJS, 255, 8, doi: [10.3847/1538-4365/abe23c](https://doi.org/10.3847/1538-4365/abe23c)
- Sainsbury-Martinez, F., Wang, P., Fromang, S., et al. 2019,
A&A, 632, A114, doi: [10.1051/0004-6361/201936445](https://doi.org/10.1051/0004-6361/201936445)
- Sarkis, P., Mordasini, C., Henning, Th., Marleau, G. D., & Mollière, P. 2021, *A&A*, 645, A79,
doi: [10.1051/0004-6361/202038361](https://doi.org/10.1051/0004-6361/202038361)
- Sato, M. 1991, *Contributions to Plasma Physics*, 31, 331,
doi: [10.1002/ctpp.2150310307](https://doi.org/10.1002/ctpp.2150310307)
- Showman, A. P., Cho, J. Y. K., & Menou, K. 2010, in
Exoplanets, ed. S. Seager, 471–516
- Tremblin, P., Chabrier, G., Mayne, N. J., et al. 2017, *ApJ*,
841, 30, doi: [10.3847/1538-4357/aa6e57](https://doi.org/10.3847/1538-4357/aa6e57)
- Wu, Y., & Lithwick, Y. 2012, *The Astrophysical Journal*,
763, 13, doi: [10.1088/0004-637x/763/1/13](https://doi.org/10.1088/0004-637x/763/1/13)
- Zhu, X., Talaat, E. R., Baker, J. B. H., & Yee, J. H. 2005,
Annales Geophysicae, 23, 3313,
doi: [10.5194/angeo-23-3313-2005](https://doi.org/10.5194/angeo-23-3313-2005)